Overcharge Protection for 4 V Lithium Batteries at High Rates and Low Temperatures

Guoying Chen[*, z] and Thomas J. Richardson[*]

Environmental Energy Technologies Division,

Lawrence Berkeley National Laboratory,

Berkeley, California 94720, USA

Abstract

Overcharge protection for 4 V $Li_{1.05}Mn_{1.95}O_4$/lithium cells at charging rates in excess of 1 mA/cm^2 (3C) and at temperatures as low as -20° C was achieved using a bilayer separator coated with two electroactive polymers. High rate and low temperature overcharge protection and discharge performance were improved by employing a design in which the polymer-coated portion of the separator is in parallel with the cell rather than between the electrodes. The effects of different membrane supports for the electroactive polymers are also examined.

---

[*] Electrochemical Society Active Member

[z] E-mail: gchen@lbl.gov

Introduction

Rechargeable lithium batteries are known for their high energy density and excellent cycle life, and they have become the dominant technology for personal electronic devices. Safety issues persist, however, with numerous unfortunate incidents reported in recent years. Overcharging has long been recognized as a primary problem, as dangerous events involving fire and explosion can result.[1] For vehicle applications (with low tolerance for hazards), series-connected cells are required to provide high voltages. Monitoring and controlling the potential of individual cells within the stack presents a severe challenge in terms of weight, volume, and cost. An alternative approach that provides reliable and inexpensive protection is needed to maintain each cell within a safe potential window. Extension of cell pack lifetime is an additional benefit.

Redox shuttle additives have been studied extensively for this purpose.[2-4] That approach is fundamentally limited, however, as it relies on diffusion of additive molecules and radical cations across the separator, resulting in low rate capability and poor low temperature performance. Because lithium ion batteries are especially susceptible to damage on overcharging at low temperatures due to high resistances in both electrodes and electrolyte,[5] and because vehicle batteries will unavoidably be exposed to low temperatures, an alternative (or additional) protection mechanism is needed.

We have previously demonstrated the use of electroactive polymers to provide overcharge protection for rechargeable lithium batteries.[6] When impregnated into a porous membrane separator, a small amount of polymer can provide self-actuated, reversible protection for cells using a variety of chemistries. Detailed characterization

and modeling of the protection mechanism has provided useful cell design parameters.[7-8] A bilayer configuration comprising a high voltage polymer composite adjacent to the cathode and low voltage polymer composite adjacent to the battery anode expands applicability to cells that operate above 4 V vs. Li.[9] Since the polymer protection approach uses electronic conduction and only a minimum of ion mobility is required to establish the internal short, it is relatively immune to limitations imposed by charging rate and low temperatures. In this paper, we demonstrate high rate capability and excellent low temperature performance of electroactive polymer overcharge protection, using an overcharge-susceptible lithium-rich spinel $Li_{1.05}Mn_{1.95}O_4$ as cathode and Li metal as anode. The bilayer separator contains a polyfluorene polymer in contact with the cathode and poly(3-butylthiophene) (P3BT) next to the anode. A modified cell configuration that lowers the internal resistance of the separator during normal operation is also described.

Experimental

Neutral poly(3-butylthiophene) (P3BT) with a 97% head-to-tail regiospecific conformation was purchased from Aldrich Chemical Co., Inc. Neutral poly(9,9-dioctylfluorene), end-capped with dimethylphenyl groups (PFO-DMP, M_w = 40,000 to 120,000) was purchased from American Dye Source, Inc. The polymers were used as received. Samples for cyclic voltammetry (CV) were prepared by dissolving PFO-DMP in chloroform and casting the solution onto a stainless steel mesh current collector (304 SS, 200 mesh). The polymer loading was 0.8 mg over a geometric area of 2.6 cm^2. The polymer-coated working electrode was mounted in a single compartment, three-electrode cell with Li metal as counter and reference electrodes.

Polymer composite separators were prepared by impregnating commercial polypropylene membranes with a 0.02 M solution of PFO-DMP or P3BT in $CHCl_3$/DMF, as described previously.[6] Three types of membrane substrates were used: Celgard 2500 microporous membrane (25 μm thick, 55% porosity), Viledon (Freudenberg) nonwoven membrane (175 μm thick, 55% porosity), and Tapyrus meltblown membrane (65 μm thick, 70% porosity) from Tapyrus Co. LTD. The polymer loading was 140 $\mu g\text{-}cm^{-2}$.

The $Li_{1.05}Mn_{1.95}O_4$ cathode laminates contained 84 wt % $Li_{1.05}Mn_{1.95}O_4$ powder (Toda M08), 4 wt % Shawinigan carbon black (Chevron), 4 wt % graphite (SFG-6, Timical) and 8 wt % polyvinylidene difluoride (PVDF) binder (Kureha) on aluminum foil. Charge-discharge cycling was carried out in "Swagelok"-type cells with $Li_{1.05}Mn_{1.95}O_4$ composite cathodes, polypropylene membranes, Li foil anodes and stainless steel current collectors. In overcharge-protected cells, polymer composite membranes were used in place of virgin polypropylene membranes. Low temperature experiments were carried out in a Thermotron environmental chamber (Model S1.2, Thermotron Industries, Inc.). The temperature was reduced from 25 °C to -20 °C in five steps, with data taken at 25 °C, 20 °C, 10 °C, 0 °C, -10 °C, and -20 °C. The cell was held at each temperature for 1 hr before testing.

The electrolyte used in the ambient temperature experiments was 1.0 M $LiPF_6$ in 1:1 propylene carbonate (PC) and ethylene carbonate (EC), and was purchased from Ferro Corporation. For the low temperature experiments, an electrolyte 1.0 M $LiPF_6$ in 1:1:3 PC, EC and dimethyl carbonate (DMC) was provided by the Army Research Laboratory. All cells were assembled in an inert atmosphere glovebox with oxygen content < 1 ppm and water < 2 ppm. X-ray diffraction (XRD) patterns were collected in

reflection mode using a Panalytical Xpert Pro diffractometer equipped with monochromatized Cu Kα radiation. The scan rate was 0.0025°/s from 10° to 70° 2θ in 0.01° steps.

Results and Discussion

Room temperature overcharge protection

Owing to their low cost, low toxicity and high rate capability, spinel-type lithium manganese oxides are among the most promising cathode materials for rechargeable lithium batteries. Because the stoichiometric spinel $LiMn_2O_4$ exhibits significant capacity fading during charge/discharge cycling, excess Li is often introduced to improve the cycling stability.[10] The electrode typically operates in a potential window of 3.5 to 4.3 V, and is quite susceptible to overcharge damage, which can result in irreversible structural changes.[11-12] To provide overcharge protection for this material without sacrificing capacity, an electroactive polymer operating just above 4 V is required.

Substituted polyfluorenes have emerged as an important class of electroactive polymers. Their efficient electroluminescence coupled with high charge carrier mobility and good processability has made them attractive for use in organic light-emitting diodes (OLEDs).[13-14] Functional characteristics of the polymers, such as intrinsic conductivity, electronic structure, chemical and electrochemical stability, and solubility in organic solvents, are adjustable through the variation of substituent groups. A range of substituted polyfluorenes is commercially available. Poly(9,9-dioctylfluorene), end-capped with dimethylphenyl groups (PFO-DMP) (Fig. 1a) was used for this study because of its good solubility in $CHCl_3$ and its measured rapid increase in electronic conductivity upon

oxidation. Fig. 1b shows a cyclic voltammogram of the polymer at room temperature. A single redox couple, reflecting oxidation/reduction of the polymer with simultaneous intercalation and deintercalation of PF_6^- anions, was observed when the potential was swept between 3.0 and 4.5 V. The onset oxidation potential was 4.15 V, suggesting that it is suitable for the protection of $Li_{1.05}Mn_{1.95}O_4$ cells. The polymer showed good stability in the electrolyte, as no changes were observed in the CV after 10 cycles.

An overcharge-protected cell, with PFO-DMP coated on Viledon nonwoven membrane as the high voltage composite separator and P3BT on Celgard 2500 membrane as the low voltage composite separator, was assembled and tested at room temperature. The nonwoven membrane (Fig. 2a) was chosen to support the high voltage polymer because it possesses a network of long polypropylene fibers and a more open pore structure compared to the microporous membrane (Fig. 2b). It allows for a uniform distribution of PFO-DMP on the internal membrane surfaces and produces a highly porous composite membrane that promotes good utilization of the electroactive polymer (Fig. 2c) and high ion conductivity in the separator. P3BT, with an onset oxidation potential of 3.2 V[6] was coated onto a Celgard microporous membrane (used to prevent lithium dendrite penetration) and placed next to the anode. The high voltage PFO-DMP composite determines the electrochemical characteristics of the internal short, while the low voltage P3BT composite protects PFO-DMF from degradation at low voltages close to the anode.

Galvanostatic charge and discharge profiles for the protected $Li_{1.05}Mn_{1.95}O_4$ - Li cell are shown in Fig. 3a. At a current density of 0.063 mA/cm^2 (C/6), the cell voltage gradually increased to 4.3 V as the $Li_{1.05}Mn_{1.95}O_4$ cathode was charged. The polymer then

began to become conductive, allowing the potential to fall very slightly as it carried most of the charging current until it reached the charging time limit. The cell was overcharged by 20% and then discharged to 3.5 V. In each cycle the polymer short was generated at the end of charging and was then removed during discharging. The protection was highly reversible, as the charge and discharge capacity of the cell remained constant for more than 20 cycles. The XRD pattern of this electrode is shown in Fig. 3b, along with that of the control electrode that was charged once to 4.3 V. The XRD patterns are essentially identical, indicating that the two electrodes were at the same state of charge (SOC), and that no structural changes had occurred in the protected electrode.

For comparison, an unprotected cell with a $Li_{1.05}Mn_{1.95}O_4$ cathode, an uncoated Celgard 2500 separator, and a Li anode was charged at a constant current density of 0.063 mA/cm^2 (C/6) and then held at 4.3 V for 5 hr to simulate the cycling profile of the protected cell. The charge-discharge performance is shown in Fig. 4a. One can see that without polymer protection, the charging current gradually decreased during the constant voltage holding at 4.3 V. The capacity of the cell faded quickly as its ability to pass current decreased due to the overcharging abuse. After the final overcharging cycle, the cell was allowed to rest for 2 h and then disassembled in the glovebox. The cathode was removed and rinsed thoroughly with DMC to remove electrolyte residue, then dried in the glovebox and examined by XRD. Fig 4b shows the XRD pattern of the charged cathode from the unprotected cell, removed after 18 cycles. Compared to a control electrode that was charged once to 4.3 V at the same charging rate of C/6, the cycled electrode shows significant peak broadening, indicating structural degradation in the material. The peaks of the spinel phase are also at lower diffraction angles compared to those from the control

electrode. Since the peaks shift continuously to higher diffraction angles with decreasing lithium content in $Li_{1.05}Mn_{1.95}O_4$,[15] this suggests that the cycled electrode is at a lower SOC than that expected at 4.3 V, possibly due to particle isolation within the electrode. Alternatively, the peak shifts may indicate structural changes at the unit cell level.

The discharge capacities of the protected and unprotected cells are shown in Fig. 5. The protected cell maintained its discharge capacity of 80 mAh/g for many cycles, while the unprotected cell quickly lost capacity due to overcharging.

Rate capability of overcharge protection

Electroactive polymers have the ability to switch rapidly between conductive and insulating states and sustain current densities as high as 300 mA/cm^2.[7] The current carrying properties of composite membranes coated with electroactive polymers are influenced by other factors, such as the loading of the polymer, the morphology of the deposited polymer, the porosity of the composite, and the availability of doping anions from the electrolyte.

Fig. 6 compares the room-temperature rate performance of a plain $Li_{1.05}Mn_{1.95}O_4$ - Li cell and a cell protected by the PFO-DMP and P3BT composite separators. Both cells were charged and discharged at current densities of 0.06 (C/6), 0.50 (1.3C), 0.63 (1.7C), 0.75 (2C) and 1.0 mA/cm^2 (2.7C), each for five cycles before moving on to the next higher rate. For the protected cell (Fig. 6a), a steady state potential was reached and maintained at each cycling rate, indicating that a short was establish and maintained by the conducting polymers. The steady state potential increased with the charging rate, resulting in increased oxidation (and electronic conductivity) of the polymers.[7] At a

current density of 1.0 mA/cm^2 (2.7 C), the separator was able to maintain a voltage of 4.6 V. In this configuration, however, a steady state potential could not be maintained above 1.0 mA/cm^2.

The voltage profile of the unprotected cell, which had its upper cutoff voltage set at the steady state potential of the protected cell for each charge/discharge rate (Fig. 6b), shows less polarization than the protected cell, especially at high rates. The capacity of the protected also cell decreased more rapidly with increasing rate. This is due to higher internal resistance in the protected cell. While the normal cell contains only a single 25 μm separator, the protected cell has two layers of coated separators with a total thickness of 200 μm.

Low temperature overcharge protection

At low temperatures, lithium metal can plate on the anode during overcharging, raising safety concerns and causing capacity losses.[16-20] Cells are also more likely to be overcharged due to the increase in cell resistance. Low temperature performance of a $Li_{1.05}Mn_{1.95}O_4$ – Li cell protected by the combination of a PFO-DMP Viledon composite and a P3BT Celgard composite is shown in Figure 7. When charged and discharged at C/6 rate (0.06 mA/cm^2), the cell was reversibly protected at each temperature, ranging from 25 °C to -20 °C. As the temperature decreased, the potential at which the short was initiated increased, mainly due to decreased ion mobility. At each temperature, the short persisted and improved with time, as more of the polymer became conducting. A significant capacity loss occurred below -10 °C, as the electrolyte began to solidify and

cell resistance increased. At -20 °C, the cell was still protected, even through the discharge capacity was very small due to the high polarization of the electrolyte.

Improved rate and low temperature performance with a modified cell configuration

To decrease the internal resistance of the protected cells, an alternative configuration (Fig. 8) with the electroactive polymers placed outside of the active electrode area was adapted. A different substrate, "Tapyrus" meltblown membrane with 70% porosity and 65 μm thickness, was also used to support the PFO-DMP polymer to better match in thickness. A $Li_{1.05}Mn_{1.95}O_4$ - Li cell was assembled with a PFO-DMP-coated Tapyrus membrane and a P3BT-coated Celgard membrane placed in parallel to the cell (in this case occupying 50% of the current collector area). Untreated Celgard was used as separator between the cathode and anode. The performance of this cell at charge/discharge current densities of 0.25 (C/1.5), 0.375 (C), 0.50 (1.3C), 0.75 (2C), 1.0 (2.7C) and 1.125 mA/cm^2 (3C) is shown in Fig. 9. The protected cell was able to reach and maintain a steady state potential for charging rates as high as 3C. Compared with the data in Fig. 6a, there is a slower increase in steady state potential with rate, and the cell was able to maintain at 3C overcharging at 4.3 V. The voltage profile also indicates lower internal resistance, and the discharge capacity remained nearly unchanged with the increasing current density.

The low temperature performance was also examined with the parallel configuration, as shown in Fig. 10. At C/6 rate, a steady state potential was reached at each temperature from 25 °C to -20 °C (Fig. 10a). Although, as before, the capacity gradually decreased with decreasing temperature, the change was less significant. The

greatest capacity reduction occurred at -20 °C, where the cell resistance increased drastically due to the increase in electrolyte viscosity. The onset protection potential increased with decreasing temperature (Fig. 10b), and the cell was protected at 4.5 V at -20 °C.

Conclusions

A bilayer configuration consisting of PFO-DMP and P3BT composite separators was used for overcharge protection in $Li_{1.05}Mn_{1.95}O_4$ – Li cells. Although this arrangement provided overcharge protection at 2.7 C and at -20 °C, substantial internal resistance and capacity losses were observed under these conditions. A modified cell configuration with polymer composites placed next to the electrode assembly was developed, which significantly lowered the internal resistance and provided overcharge protection at a rate up to 3C. The capacity loss at high rate and low temperatures were also significantly lower.

Acknowledgements

We thank Celgard Inc., Freudenberg and Tapyrus Co. LTD for providing membranes. This work was supported by the Assistant Secretary for Energy Efficiency and Renewable Energy, Office of Vehicle Technologies of the U.S. Department of Energy under Contract No. DE-AC02-05CH11231.

References

[1] S. R. Narayanan, S. Surampudi, A. I. Attia, and C. P. Bankston, *J. Electrochem. Soc.*, **138**, 2224 (1991).

[2] T. J. Richardson and P. N. Ross, *J. Electrochem. Soc.*, **143**, 3992 (1996).

[3] M. Adachi, K. Tanaka, and K. Sekai, *J. Electrochem. Soc.*, **146**, 1256 (1999).

[4] J. Chen, C. Buhrmester, and J. R. Dahn, *Electrochem. Solid-State Lett.*, **8**, A59 (2005).

[5] M. S. Ding, K. Xu, S. S. Zhang, K. Amine, G. L. Henriksen, and T. R. Jow, *J. Electrochem. Soc.*, **148**, A1196 (2001).

[6] G. Chen and T. J. Richardson, *Electrochem. Solid-State Lett.*, **9**, A24 (2006).

[7] G. Chen, K. E. Thomas-Alyea, J. Newman, and T. J. Richardson, *Electrochim. Acta.*, **50**, 4666 (2005).

[8] K. E. Thomas-Alyea, J. Newman, G. Chen, and T. J. Richardson, *J. Electrochem. Soc.*, **151**, A509 (2004).

[9] G. Chen and T. J. Richardson, *Electrochemical and Solid State Letters*, **9**, A24 (2006).

[10] Y. Gao and J. R. Dahn, *J. Electrochem. Soc.*, **143**, 825 (1996).

[11] J. M. Tarascon, W. R. Mckinnon, F. Coowar, T. N. Bowmer, G. Amatucci, and D. Guyomard, *J. Electrochem. Soc.*, **141**, 1421 (1994).

[12] S. J. Wen, T. J. Richardson, L. Ma, K. A. Striebel, P. N. Ross, and E. J. Cairns, *J. Electrochem. Soc.*, **143**, L136 (1996).

[13] Y. Kervella, M. Armand, and O. Stéphan, *J. Electrochem. Soc.*, **148**, H155 (2001).

[14] K.-H. Weinfurtner, H. Fujikawa, S. Tokito, and Y. Taga, *Appl. Phys. Lett.*, **76**, 2502 (2000).

[15] H. Huang, C. A. Vincent, and P. G. Bruce, *J. Electrochem. Soc.*, **146**, 3649 (1999).

[16] J. Fan and S. Tan, *J. Electrochem. Soc.*, **153,** A1081 (2006).

[17] H.-P. Lin, D. Chua, M. Salomon, H.-C. Shiao, M. Hendrickson, E. Plichta, and S. Slane, *Electrochem. Solid State Lett.*, **4,** A71 (2001).

[18] M. C. Smart, B. V. Ratnakumer, L. Whitcanack, K. Chin, M. Rodriguez, and S. Surampudi, *IEEE Aerospace Electronic Systems Magazine*, **17**, 16 (2002).

[19] A. N. Jansen, D. W. Dees, D. P. Abraham, K. Amine, and G. L. Henriksen, *J. Power Sources*, **174,** 373 (2007).

[20] S. S. Zhang, K. Xu, and T. R. Jow, *J. Power Sources*, **160,** 1349 (2006).

Figure captions

Figure 1. a) structure of PFO-DMP; b) cyclic voltammogram of PFO-DMP in 1.0 M $LiPF_6$ in 1:1 EC: PC. Scan rate 5 mV s^{-1}, Li foil counter and reference electrodes.

Figure 2. SEM images of a) Viledon nonwoven membrane; b) Celgard 2500 membrane; c) PFO-DMP impregnated Viledon membrane.

Figure 3. a) charge-discharge cycling of a $Li_{1.05}Mn_{1.95}O_4$ - Li cell protected with a PFO-DMP Viledon composite and a P3BT Celgard composite; b) XRD patterns of $Li_{1.05}Mn_{1.95}O_4$ electrodes.

Figure 4. a) charge-discharge cycling of an unprotected $Li_{1.05}Mn_{1.95}O_4$ - Li cell; b) XRD patterns of $Li_{1.05}Mn_{1.95}O_4$ electrodes. * indicates peaks from Al sample holder.

Figure 5. Cycling performance of the protected and unprotected $Li_{1.05}Mn_{1.95}O_4$ - Li cells.

Figure 6. Rate performance of $Li_{1.05}Mn_{1.95}O_4$ - Li cells: a) protected with a PFO-DMP Viledon composite and a P3BT Celgard composite; b) unprotected.

Figure 7. Low temperature performance of a $Li_{1.05}Mn_{1.95}O_4$ - Li cell protected with a PFO-DMP Viledon composite and a P3BT Celgard composite.

Figure 8. Modified cell configurations for overcharge protection.

Figure 9. Rate performance of a protected $Li_{1.05}Mn_{1.95}O_4$ - Li cell with the new cell configuration.

Figure 10. a) low temperature performance of a protected $Li_{1.05}Mn_{1.95}O_4$ - Li cell with the new cell configuration; b) onset protection potential at different temperatures.

Figure 1

a)

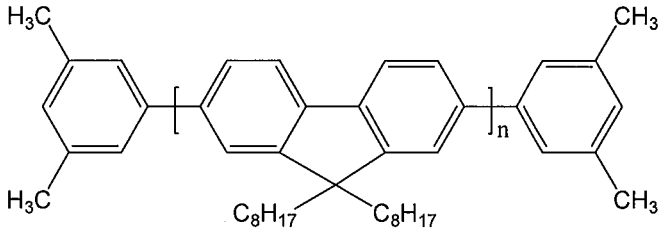
H3C
CH3
n
H3C
CH3
C8H17
C8H17

b)

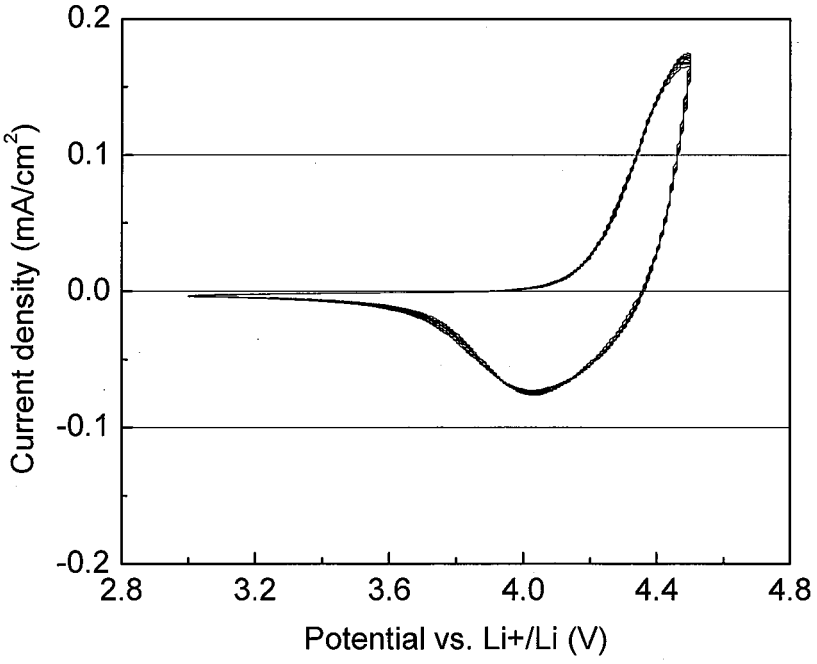
0.2
0.1
0.0
-0.1
-0.2
Current density (mA/cm2)
2.8
3.2
3.6
4.0
4.4
4.8
Potential vs. Li+/Li (V)

Figure 2

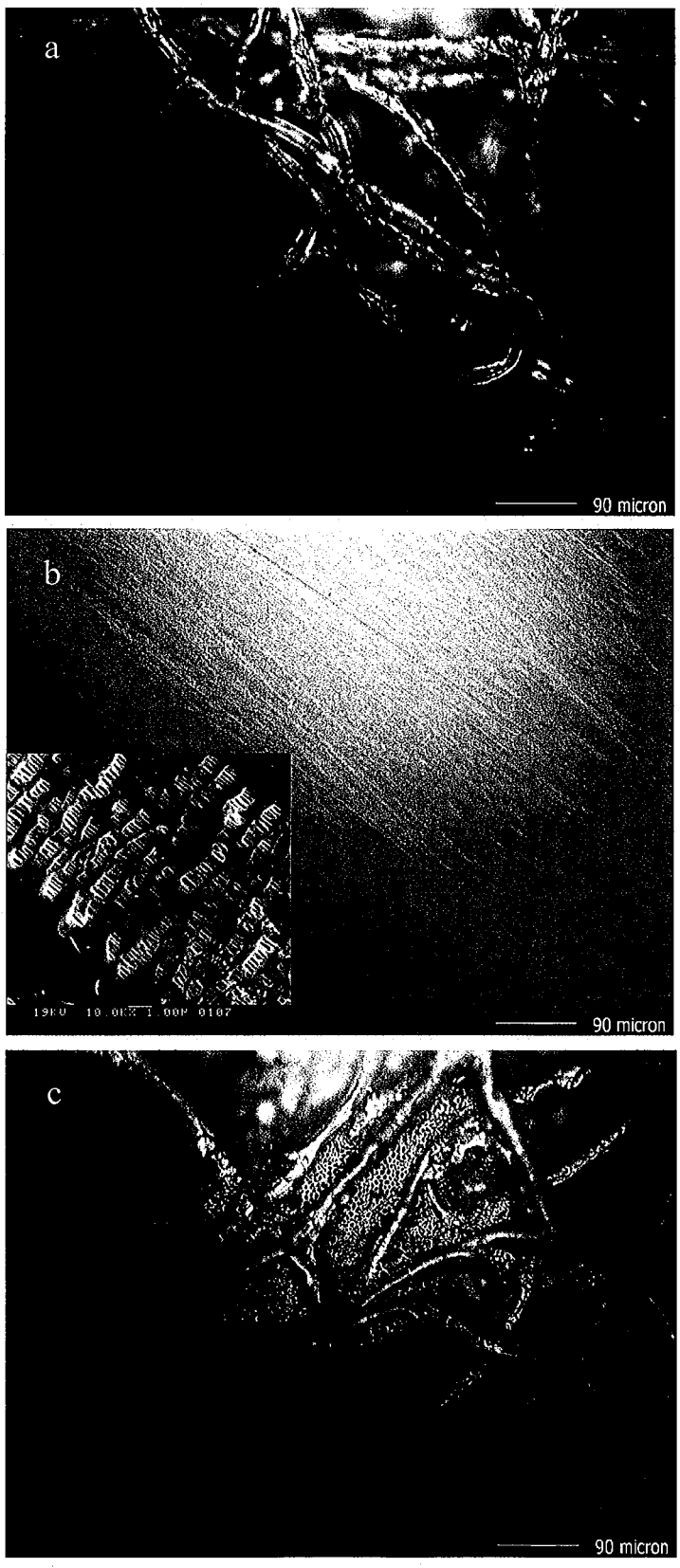

Figure 3

a)

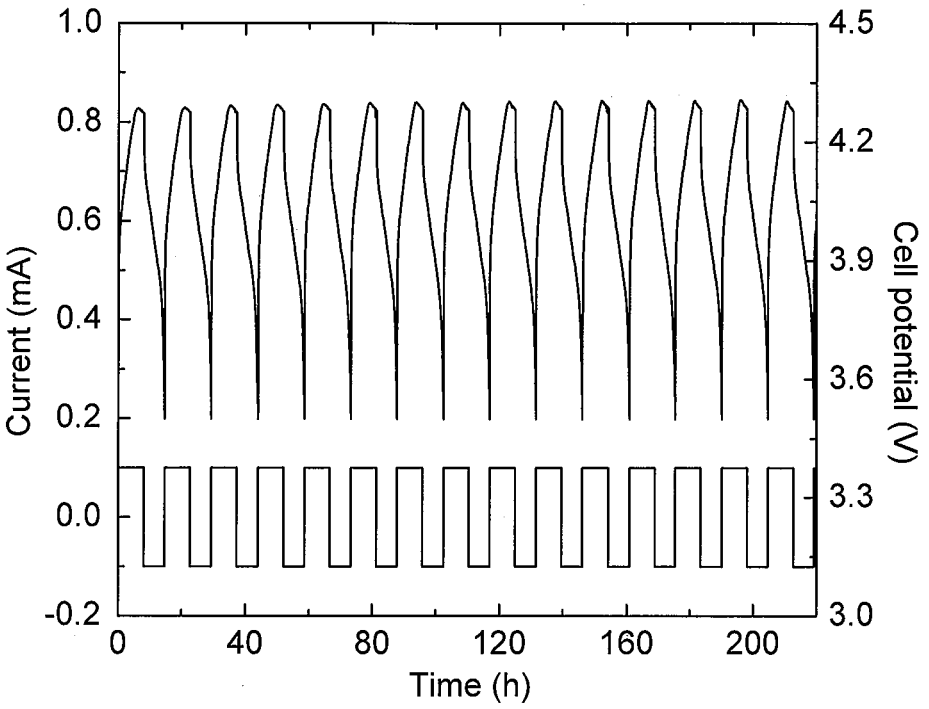
1.0
0.8
0.6
0.4
0.2
0.0
-0.2
Current (mA)
4.5
4.2
3.9
3.6
3.3
3.0
Cell potential (V)
0
40
80
120
160
200
Time (h)

b)

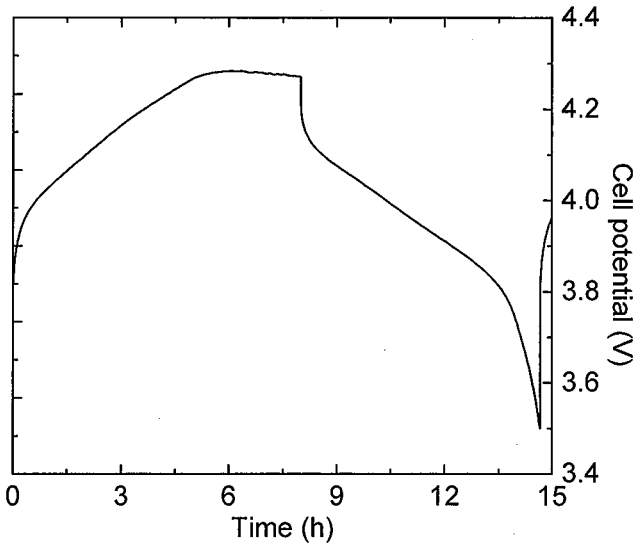
4.4
4.2
4.0
3.8
3.6
3.4
Cell potential (V)
0
3
6
9
12
15
Time (h)

c)

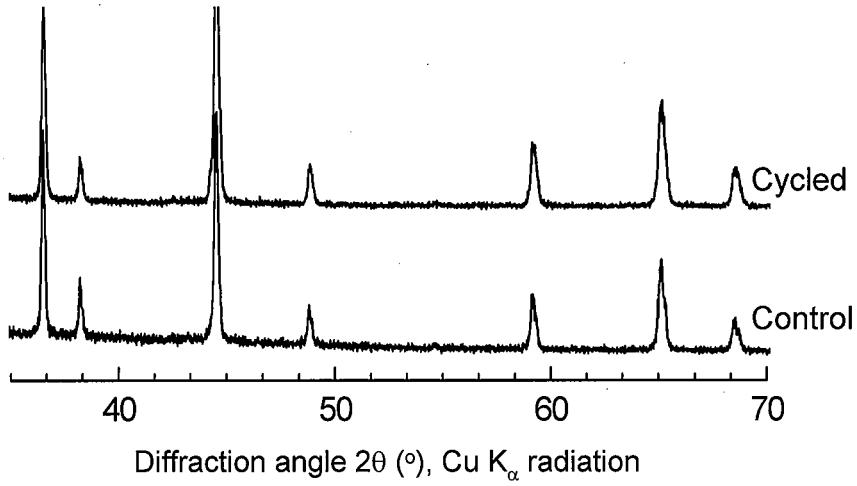
Cycled
Control
40
50
60
70
Diffraction angle 2θ (°), Cu K_α radiation

Figure 4

a)

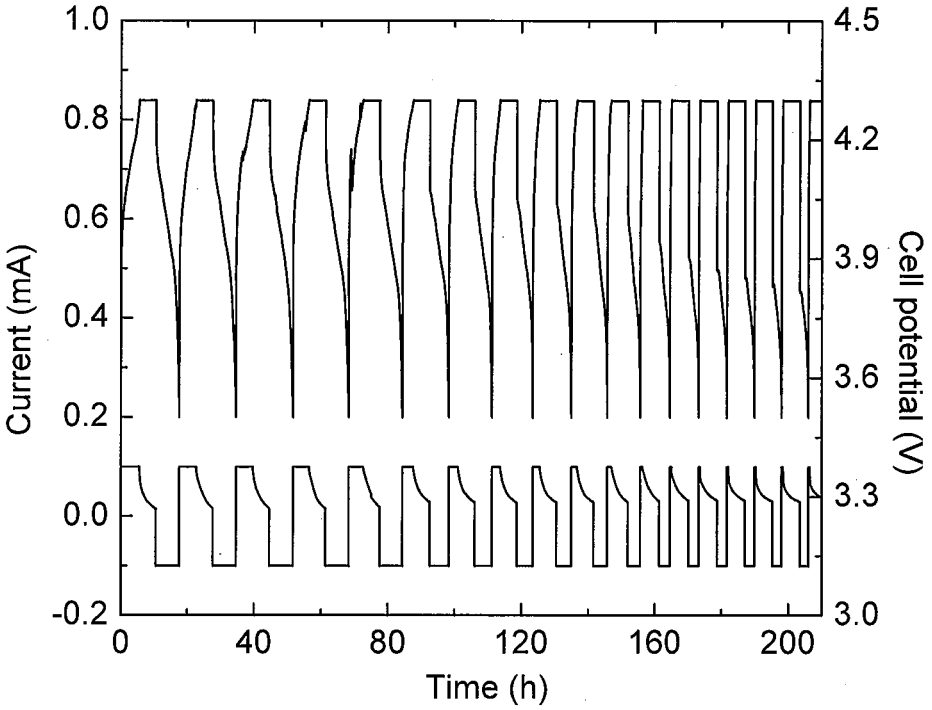
1.0
0.8
0.6
0.4
0.2
0.0
-0.2
Current (mA)
4.5
4.2
3.9
3.6
3.3
3.0
Cell potential (V)
0
40
80
120
160
200
Time (h)

b)

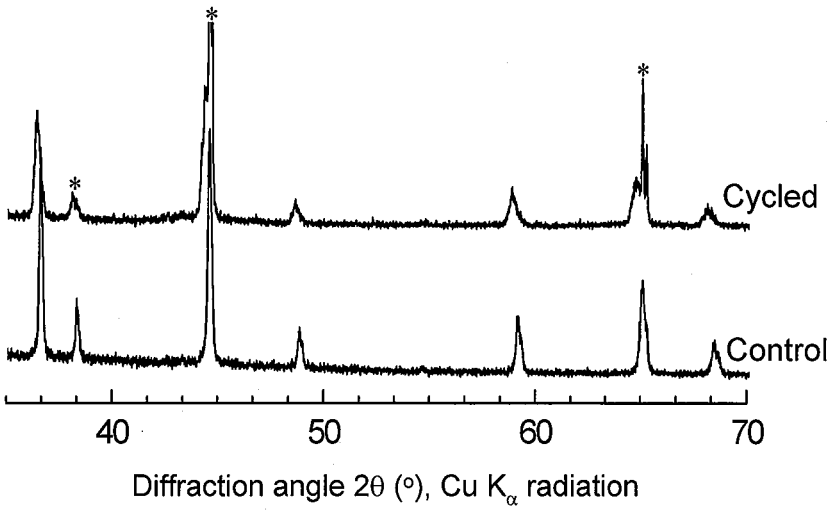
*
*
*
Cycled
Control
40
50
60
70
Diffraction angle 2θ (°), Cu Kα radiation

Figure 5

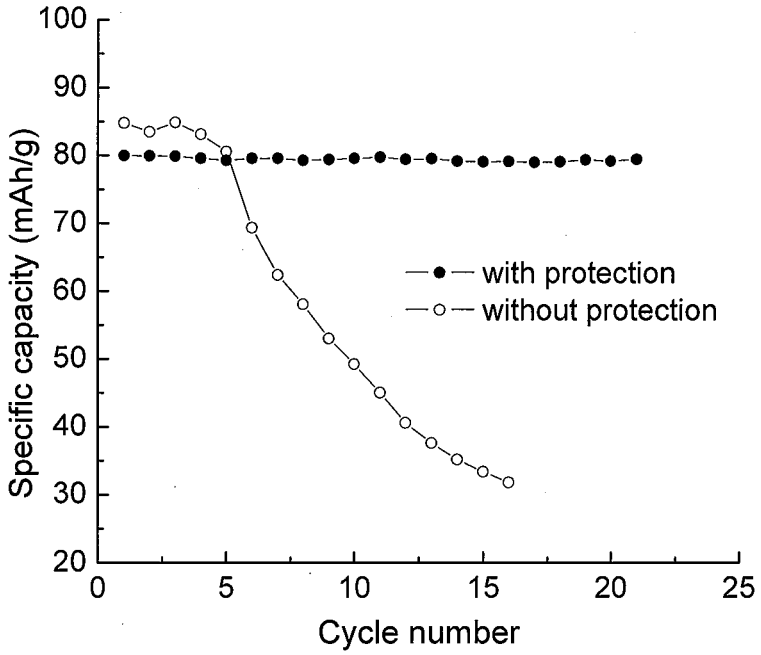
100
90
80
70
60
50
40
30
20
Specific capacity (mAh/g)
0
5
10
15
20
25
Cycle number
with protection
without protection

Figure 6

a)

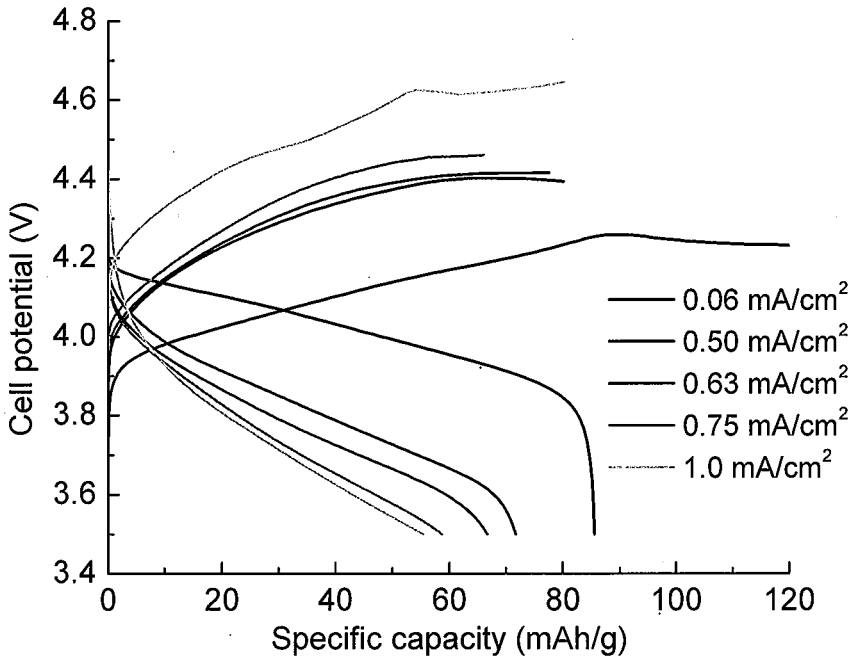
4.8
4.6
4.4
4.2
4.0
3.8
3.6
3.4
Cell potential (V)
0
20
40
60
80
100
120
Specific capacity (mAh/g)
0.06 mA/cm2
0.50 mA/cm2
0.63 mA/cm2
0.75 mA/cm2
1.0 mA/cm2

b)

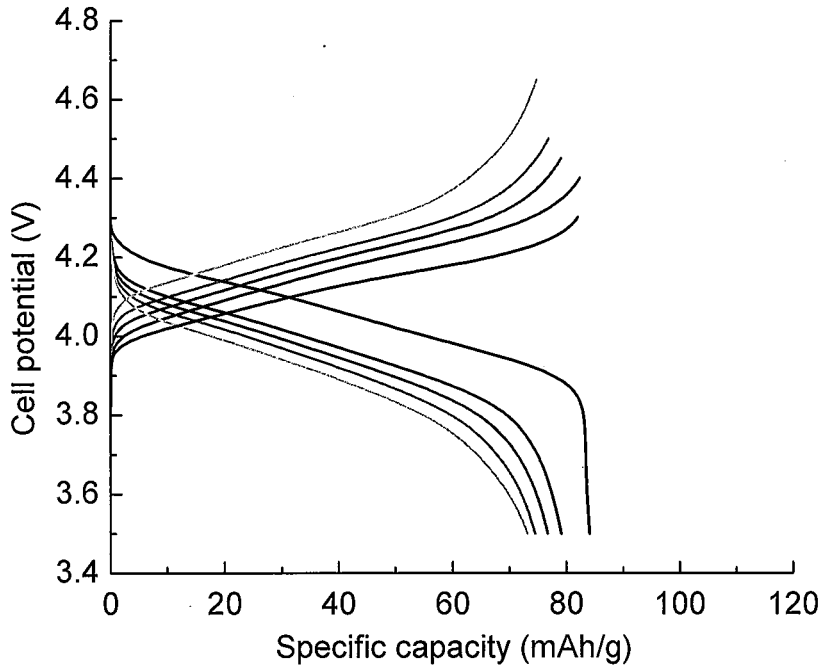
4.8
4.6
4.4
4.2
4.0
3.8
3.6
3.4
Cell potential (V)
0
20
40
60
80
100
120
Specific capacity (mAh/g)

Figure 7

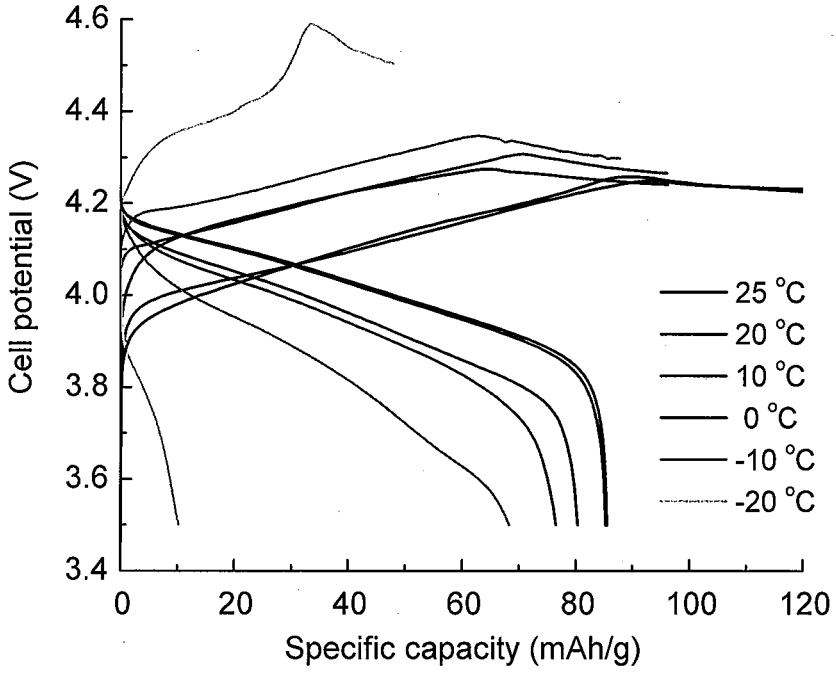
4.6
4.4
4.2
4.0
3.8
3.6
3.4
Cell potential (V)
0
20
40
60
80
100
120
Specific capacity (mAh/g)
25 °C
20 °C
10 °C
0 °C
-10 °C
-20 °C

Figure 8

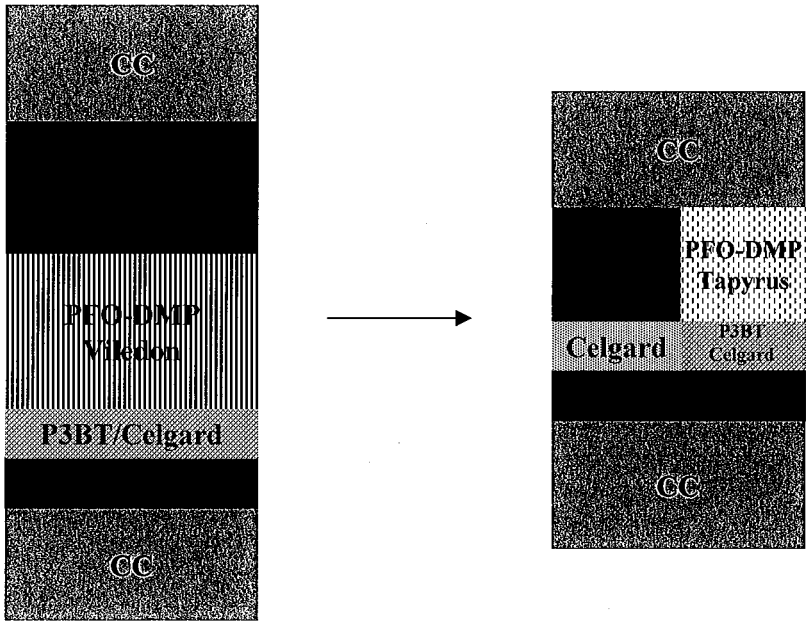
CC
PFO-DMP
Vikelon
P3BT/Celgard
CC
CC
PFO-DMP
Tapyrus
Celgard
P3BT
Celgard
CC

Figure 9

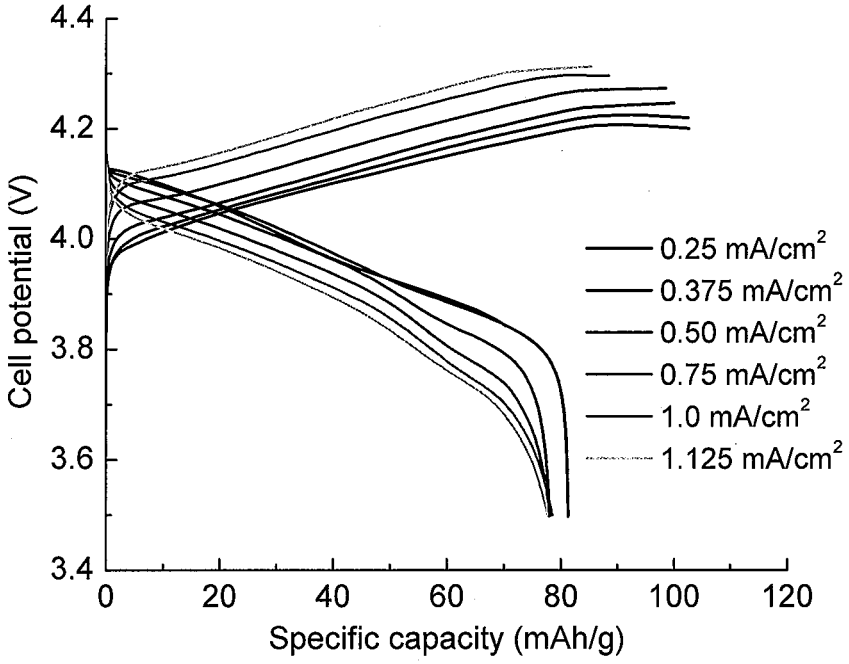
4.4
4.2
4.0
3.8
3.6
3.4
Cell potential (V)
0
20
40
60
80
100
120
Specific capacity (mAh/g)
0.25 mA/cm2
0.375 mA/cm2
0.50 mA/cm2
0.75 mA/cm2
1.0 mA/cm2
1.125 mA/cm2

Figure 10

a)

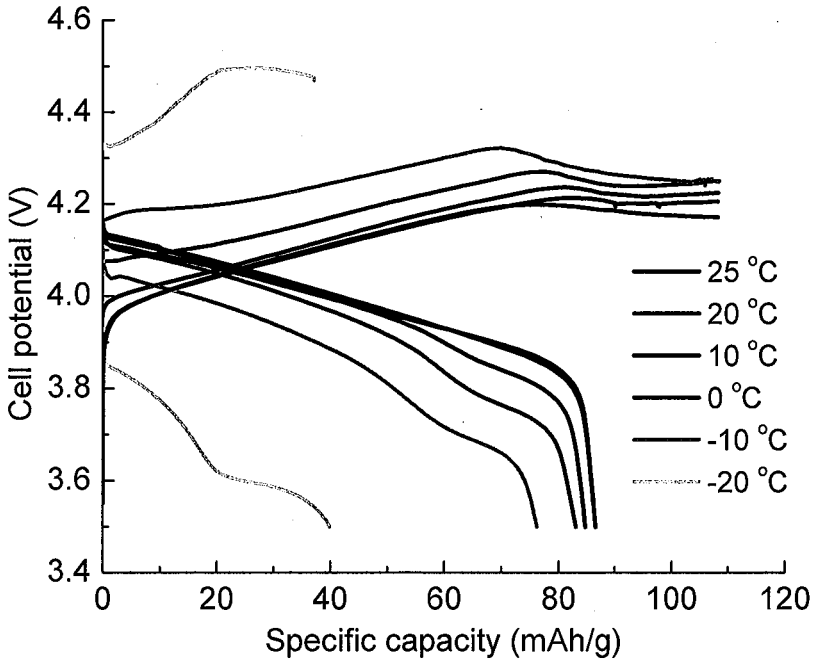
4.6
4.4
4.2
4.0
3.8
3.6
3.4
Cell potential (V)
0
20
40
60
80
100
120
Specific capacity (mAh/g)
25 °C
20 °C
10 °C
0 °C
-10 °C
-20 °C

b)

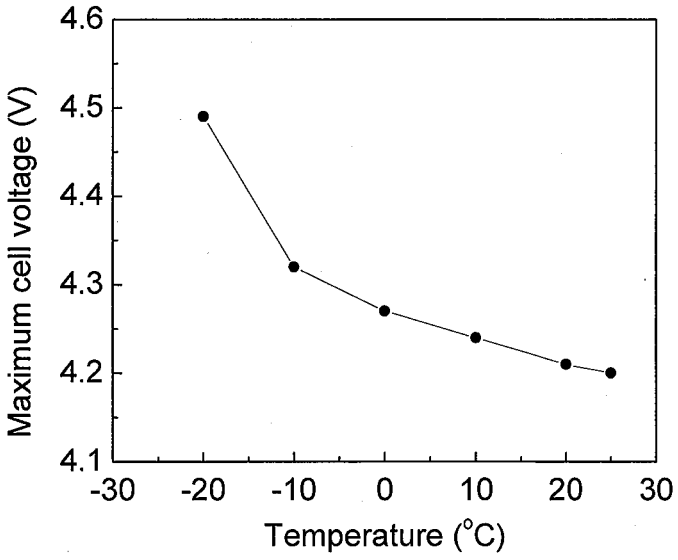
4.6
4.5
4.4
4.3
4.2
4.1
Maximum cell voltage (V)
-30
-20
-10
0
10
20
30
Temperature (°C)